Atta, Khalid Tourkey; Hostettler, Roland; Birk, Wolfgang; Johansson, Andreas

Phasor extremum seeking control with adaptive perturbation amplitude

Published in:
2016 IEEE 55th Conference on Decision and Control (CDC)

DOI:
10.1109/CDC.2016.7799358

Published: 27/12/2016

Document Version
Peer-reviewed accepted author manuscript, also known as Final accepted manuscript or Post-print

Please cite the original version:
Atta, K. T., Hostettler, R., Birk, W., & Johansson, A. (2016). Phasor extremum seeking control with adaptive perturbation amplitude. In *2016 IEEE 55th Conference on Decision and Control (CDC)* (pp. 7069-7074). Article 7799358 (Proceedings of the IEEE Conference on Decision & Control). IEEE. https://doi.org/10.1109/CDC.2016.7799358

Phasor Extremum Seeking Control with Adaptive Perturbation Amplitude

Khalid T. Atta, Roland Hostettler, Wolfgang Birk,
and Andreas Johansson

This is a post-print of a paper published in *55th IEEE Annual Conference on Decision and Control (CDC)*. When citing this work, you must always cite the original article:

K. T. Atta, R. Hostettler, W. Birk, and A. Johansson, “Phasor extremum seeking control with adaptive perturbation amplitude,” in *55th IEEE Annual Conference on Decision and Control (CDC)*, Las Vegas, NV, USA, December 2016

DOI

10.1109/CDC.2016.7799358

Phasor Extremum Seeking Control with Adaptive Perturbation Amplitude

Khalid Tourkey Atta⋆, Roland Hostettler†, Wolfgang Birk⋆, and Andreas Johansson⋆

Abstract— **In this paper, we propose a perturbation amplitude adaption scheme for phasor extremum seeking control based on the plant's estimated gradient. By using phasor extremum seeking instead of classical extremum seeking, the problem of algebraic loops in the controller formulation is avoided. Furthermore, a stability analysis for the proposed method is provided, which is the first stability analysis for extremum seeking controllers using adaptive amplitudes. The proposed method is illustrated using numerical examples and it is found that changes in optimum can be tracked accurately while the steady-state perturbations can be reduced significantly.**

I. INTRODUCTION

Extremum Seeking Control (ESC) is a data-driven, model-free control approach whose goal is to maximize (or minimize) an objective of a controlled plant. Typical applications of ESC include desalination plants, anti-lock braking systems, or maximum power point tracking in, for example, solar and hydro power, see [1] for more details. The extremum of the controlled plant is found by first superimposing a small perturbation signal, for example a sinusoid, on top of the control signal in order to estimate the gradient of the control objective with respect to the control signal. Then, the control signal is adjusted according to the found gradient [2].

The first ESC method, known as the band pass filter approach, is based on the steepest descent method. It uses a low pass filter, a multiplier, and a high pass filter to estimate the gradient [2]. Another approach, based on Newton-Raphson optimization, tries to drive the system into optimum by estimating both the gradient and Hessian [3]. Recently, a phasor-based ESC approach was proposed in [4], [5]. Here, the phasor, which is proportional to the gradient, is estimated using a Kalman filter and then used to drive the system into optimality. In general, all methods have in common that the extremum seeking dither signal is applied to the plant continuously. This clearly is a disadvantage as it causes unnecessary variation and control action around the optimal point of operation once the extremum is found. In practice, one could actually remove, or at least minimize, the applied disturbance in order to avoid these variations. Hence, in this article, we propose phasor ESC using an adaptive amplitude in the perturbation signal where the amplitude is a function of the gradient. Intuitively, this can be understood as follows. As long as the gradient is large, that is, the current input is far from the optimum, we apply large excitations in order to move quickly to the optimal point. As the working point closes in on the optimum point, the gradient decreases and hence, the excitation is also decreased.

The concept of adaptive amplitude in ESC is not entirely new. In [6], Tan et. al. proposed to decrease the excitation amplitude continuously as the extremum seeking gets closer to the optimal point. However, the adaption rule therein is based on continuously decreasing the amplitude based on a predefined decay rate. This has the disadvantage that the controller will not be able to respond adequately to changes in the optimal operation point. Futhermore, because of the rate of adaption is to be chosen by the operator, good knowledge is required to make sure that the controller reaches the optimum in practical time. Another approach, called Dither Signal Amplitude Schedule, for adapting the excitation amplitude was presented in [3]. This approach is based on Newton-like ESC and the adaption rule depends on the ratio between the estimated gradient and Hessian. A major disadvantages of this method is that the variable that will adjust the amplitude, in this case the ratio between the gradient and the Hessian, is a function of the perturbation amplitude itself which may lead to spurious adjustments.

In contrast, the method proposed here tries to address these issues. Specifically, we propose adaptive phasor extremum seeking control based on the gradient estimation independent of the perturbation amplitude, which avoids the drawback mentioned above. Also, unlike the approach in [6], it enables tracking of the optimal point even after the initial convergence phase since the amplitude can adapt if the optimal point changes. Furthermore, semi-global practical asymptotic stability (SPA) of the proposed method is proven, which is, to the best of our knowledge, the first stability proof of extremum seeking control with adaptive perturbation amplitude.

The remainder of this article is as follows. The problem is formalized in Section II followed by a brief introduction to SPA in Section III. The proposed method is shown in Section IV and its stability is proven in Section V. Section VI provides numerical illustrations of the proposed method. Concluding remarks and a discussion of future work follow in Section VII.

II. PROBLEM FORMULATION

Consider a non-linear, time varying plant with a single control objective (sometimes also called index) that can be

Funding received from the Horizon 2020 Research Programme of the European Commission under the grant number 649796 (www.opti2020.eu) (K.A. and W.B.), and financial support of the Academy of Finland (R.H.) is hereby gratefully acknowledged.

⋆Khalid T. Atta, Wolfgang Birk, and Andreas Johansson are with the Control Engineering Group, Department of Computer Science, Electrical and Space Engineering, Luleå University of Technology, Luleå, Sweden. E-mail: firstname.lastname@ltu.se.

†Roland Hostettler is with the Department of Electrical Engineering and Automation, Aalto University, Espoo, Finland. E-mail: roland.hostettler@aalto.fi.

described by the following state space representation:

$$\frac{\mathrm{d}\mathbf{x}}{\mathrm{d}t} = \mathbf{f}(\mathbf{x},\mathbf{u}) \tag{1a}$$
$$y = h(\mathbf{x}) \tag{1b}$$

In (1), $\mathbf{x} \in \mathbb{R}^n$ is a vector representing the state variables, with initial state $\mathbf{x}(0) = \mathbf{x_0}$, $\mathbf{u} \in \mathbb{R}^m$ is the manipulated (input) variables of the plant, and $y \in \mathbb{R}$ is a scalar representing the output objective (or index) of the plant. Both $\mathbf{f} : \mathbb{R}^n \times \mathbb{R}^m \to \mathbb{R}^n$ and $h : \mathbb{R}^n \to \mathbb{R}$ are assumed to be sufficiently smooth. Furthermore, the steady-state output as a function of a constant input is assumed to have a minimum (or maximum). Without loss of generality, we will assume the latter case and then the objective of the ESC controller is to adjust $\mathbf{u}$ such that the maximum value in y for any given $\mathbf{x_0}$ is attained.

Similar to the general approach in [7], we assume that the input is parametrized by θ with the control law $u = \gamma(\mathbf{x},\theta)$. Furthermore, we make the following assumptions.

Assumption 1: There exists a smooth function $l : \mathbb{R} \to \mathbb{R}^m$ such that $\mathbf{f}(\mathbf{x},\gamma(\mathbf{x},\theta)) = 0$ if and only if $\mathbf{x} = l(\theta)$.

Assumption 2: For each $\theta \in \mathbb{R}$ the equilibrium $x = l(\theta)$ of the system $\dot{x} = \mathbf{f}(x,\alpha(x,\theta))$ is globally asymptotically stable uniformly in θ.

Also, let us define $(h \circ l)(\theta) = Q(\theta)$, then our third assumption is:

Assumption 3: There exists a $\theta^* \in \mathbb{R}$ such that:

$$\frac{\partial}{\partial\theta} Q(\theta^*) = 0 \tag{2a}$$
$$(\theta - \theta^*)\frac{\partial}{\partial\theta} Q(\theta) < 0 \quad \forall \quad \theta \neq \theta^* \tag{2b}$$

From Assumption 3, it follows that $Q(\theta)$ is strictly increasing for $\theta \leq \theta^*$ and strictly decreasing for $\theta \geq \theta^*$ which ensures a unique maximum at $\theta = \theta^*$. This is even true without the assumption that $\frac{\partial^2}{\partial\theta^2} Q(\theta^*) < 0$.

III. Semi-global Practical Asymptotic Stability

First, let us define the semi-global practical asymptotic (SPA) stability of a dynamic system as defined in [7]. For definitions of comparison functions (class $\mathscr{KL}$ functions), please refer to [8, Sec. 4.4].

Definition 1: The system

$$\dot{\mathbf{x}} = \mathbf{f}(t,\mathbf{x},\varepsilon) \tag{3}$$

where $\mathbf{x} \in \mathbb{R}^n$, $t \in \mathbb{R} \geq 0$ and $\varepsilon = (\varepsilon_1, \varepsilon_2, \ldots, \varepsilon_l) \in \mathbb{R}^n_{>0}$ is said to be SPA stable, uniformly in $(\varepsilon_1, \ldots, \varepsilon_j)$, $j \in \{1, \ldots, l\}$, if there exists $\beta \in \mathscr{KL}$ such that the following holds. For each pair of strictly positive real numbers (Δ, ψ), there exist real numbers $\varepsilon_k^* = \varepsilon_k^*(\Delta,\psi) > 0, k = 1,2,\ldots,j$ and for each fixed $\varepsilon_k \in (0,\varepsilon_k^*), k = 1,2,\ldots,j$, there exist $\varepsilon_i = \varepsilon_i(\varepsilon_1,\varepsilon_2,\ldots,\varepsilon_{i-1},\Delta,\psi)$, with $i = j+1, j+2, \ldots, l$, such that the solutions of the system with the so constructed parameters ε satisfy:

$$|\mathbf{x}(t)| \leq \beta\left(|\mathbf{x}_0|,(t-t_0)\right) + \psi \tag{4}$$

for all $t \geq t_0$, $\mathbf{x}(t_0) = \mathbf{x}_0$ with $|\mathbf{x}_0| \leq \Delta$. Furthermore, if $j = l$, then we say that the system is SPA stable, uniformly in ε.

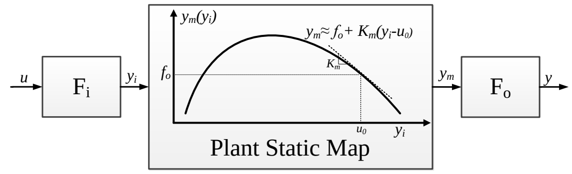

Fig. 1. The non-linear dynamic plant approximated into linear input dynamics, non linear static, and linear output dynamics parts

The SPA stability concept can be understood as follows. Given that it is required to bring a system from any given initial condition inside Δ into a convergence zone ψ, the parameters ε can be chosen such that the bounds on the "uniform" parameter $(\varepsilon_1, \ldots, \varepsilon_j)$ depend only on Δ and ψ while the "non-uniform" parameters $\varepsilon_i, i = j+1, \ldots, l$ are allowed to depend also on the other parameters $(\varepsilon_1, \ldots, \varepsilon_{i-1})$.

IV. Proposed Approach

For the demonstration of the proposed approach, and without loss of generality, we will approximate our system as a Wiener-Hammerstein model, that is, linear input and output dynamics with a non-linearity in between [3], [4], [9] as illustrated in Fig. 1. Note that this approximation is for illustration only and will not be used in the stability analysis provided in Section V.

We assume that the steady-state gain of the input and output dynamics ($F_i(0)$ and $F_o(0)$, respectively) both are equal to one. Note that if the gain is not unity, it can be adjusted and re-scaled together with the non-linear element. Further, we denote the input and output dynamics gain at the perturbation frequency ω by K_i and K_o, respectively, and the corresponding phase shifts by ϕ_i and ϕ_o, respectively. We consider the plant input to be $u(t) = u_0 + a_p \sin(\omega t)$ and assume u_0 to be almost constant during the cycle. The non-linear map of the plant when approximated using a first order Taylor series as shown in Fig. 1 can be written as $y_m = f_0 + K_m(y_i - u_o)$ where $K_m = \left.\frac{\partial y_m(t)}{\partial u(t)}\right|_{u=u_0}$. The output of the plant y will be

$$\begin{aligned} y(t) &\approx f_0 + a_p K_o K_m K_i \sin(\omega t + \phi_i + \phi_o) \\ &= \beta_0 + \alpha_1 a_p \sin(\omega t) + \beta_1 a_p \cos(\omega t) \end{aligned} \tag{5}$$

where $\beta_0 = f_0$, $\alpha_1 = K_o K_m K_i \cos\phi_i + \phi_o$, and $\beta_1 = K_o K_m K_i \sin\phi_i + \phi_o$.

Eq. (5) is a Fourier series approximation of the output, and it is assumed that the coefficients of this series can be represented by a Gaussian random walk process [10] which is a common approach to represent time series signals [11]. We can thus write $y(t)$ as the output of a linear, time-varying state-space system with state vector $\mathbf{z} = \begin{bmatrix}\beta_0 & \alpha_1 & \beta_1\end{bmatrix}^T$, as

$$\begin{aligned} \dot{\mathbf{z}}(t) &= A\,\mathbf{z}(t) + \mathbf{w}(t) \\ y(t) &= C(\omega t)\mathbf{z}(t) + v(t) \end{aligned} \tag{6}$$

where $\mathbf{w}(t)$ and $v(t)$ are mutually independent disturbances with $Q = qI$ and $R = r$ as their respective covariances [4] while A is a 3×3 matrix of zeros and $C(\omega t)$ is given by

$$C(\omega t) = \begin{bmatrix}1 & a_p \sin(\omega t) & a_p \cos(\omega t)\end{bmatrix}. \tag{7}$$

The system is observable and thus, $\mathbf{z}$ can be estimated using many methods such as the discrete time Kalman filter [12] or the periodogram [13]. In general, it is possible to use a state observer with time varying feedback

$$L(t)=\sqrt{\frac{q}{r}}L_n(\omega t)=\sqrt{\frac{q}{r}}\begin{bmatrix}1\\ \sqrt{2}\sin(\omega t+\zeta)\\ \sqrt{2}\cos(\omega t+\zeta)\end{bmatrix} \tag{8}$$

where ζ can be derived by finding the steady-state periodic solution of the continuous-time Kalman filter similar to the work in [4] or it can be left as a tuning parameter of the time-varying state observer.

Remark 1: It is important to note that the proposed approach is slightly different from the original phasor ESC presented in [4], [14]. Here, the state vector $\mathbf{z}=\begin{bmatrix}\beta_0 & \alpha_1 & \beta_1\end{bmatrix}^T$ does not depend on the perturbation amplitude a_p. This will be key in avoiding the algebraic loop encountered in [3] when adapting a_p.

With Remark 1 in mind, we could, in principle, use the fact that

$$\sqrt{\alpha_1^2+\beta_1^2}=|K_oK_mK_i|\propto|\frac{\partial y_m(t)}{\partial u(t)}|$$

and make the amplitude of the perturbation signal proportional to $\sqrt{\alpha_1^2+\beta_1^2}$. The main problem, however, is the radial unboundedness of $\sqrt{\alpha_1^2+\beta_1^2}$ which can cause big values in a_p. Instead, we suggest to use

$$\rho(\alpha_1,\beta_1)=\frac{2}{\pi}\tan^{-1}\left(\sqrt{\alpha_1^2+\beta_1^2}\right). \tag{9}$$

Remark 2: Note that $\rho(\alpha_1,\beta_1)$ is a continuous function with $\rho(\alpha_1,\beta_1)\approx\frac{2}{\pi}\left(\sqrt{\alpha_1^2+\beta_1^2}\right)$ for a small α_1 and β_1 and $\rho(\alpha_1,\beta_1)\approx 1$ for relatively large values.

Thus, similarly to [3], we suggest the adaptive amplitude adjustment as

$$\dot{a}=-\lambda a+\lambda K_g\rho(\alpha_1,\beta_1). \tag{10}$$

Further, in order to avoid singularities, we will adjust the perturbation amplitude to be

$$a_p=a_0+a^2 \tag{11}$$

where a_0 represent the minimum amplitude when the system has converged to the optimum.

The proposed ESC method can now be summarized as:

$$\frac{\mathrm{d}\mathbf{z}}{\mathrm{d}t}=\sqrt{\frac{q}{r}}L_g(\omega t)y(t)-\sqrt{\frac{q}{r}}L_n(\omega t)C(\omega t)\mathbf{z} \tag{12a}$$

$$\frac{\mathrm{d}\theta}{\mathrm{d}t}=kz_2 \tag{12b}$$

$$\frac{\mathrm{d}a}{\mathrm{d}t}=-\lambda a+\lambda K_g\rho(z_2,z_3) \tag{12c}$$

with the input to the plant being

$$\theta+a_p\sin(\omega t)=\theta+(a_0+a^2)\sin(\omega t). \tag{12d}$$

Note that in the original phasor ESC, we have that $L_g=L_n$. However, since the convergence error $\lim_{t\to\infty}(\theta-\theta^*)$ is dependent on the perturbation amplitude [9], increasing a_p will reduce the accuracy of our controller. Thus, the high accuracy phasor ESC presented in [15] will be adopted which uses

$$L_g(\omega t)=\begin{bmatrix}1\\ \sqrt{2}\left(\cos(\zeta)\,\bar{g}(\omega t)+\sin(\zeta)\,\bar{g}_c(\omega t)\right)\\ \sqrt{2}\left(\cos(\zeta)\,\bar{g}_c(\omega t)-\sin(\zeta)\,\bar{g}(\omega t)\right)\end{bmatrix}$$

where $\bar{g}(\sigma)=\sum_{m=0}^{\bar{m}}(2m+1)\sin((2m+1)\sigma)$ and $\bar{g}_c(\sigma)=\bar{g}(\sigma+\pi/2)$. Also note that choosing $\bar{g}(\omega t)=\sin(\omega t)$ gives $L_g(\omega t)=L_n(\omega t)$ as in the traditional phasor ESC algorithm. The advantage of using the modified modulation signal $\bar{g}(t)$ is that

$$\int_0^{2\pi}Q(\theta+(a^2+a_0)\sin(\sigma))\bar{g}(\sigma)\mathrm{d}\sigma=\pi(a^2+a_0)Q'(\theta) \tag{13}$$

for a sufficiently large $\bar{m}$ as shown in [15], which means the exact (scaled) gradient will be found independent of the perturbation amplitude. This will remove the convergence error as we stated earlier.

Remark 3: It can be shown that if the steady state map is a quadratic function, then $\bar{m}$ can be chosen to be zero, and the Eq. (13) still hold. For the general case, see [15, pp. 4] for a discussion on how the choice of $\bar{m}$ affects the convergence speed as well as the accuracy of the Taylor series expansion.

V. Stability analysis

We start the stability analysis by rewriting and combining the equations of the general non-linear system (1) with the equations of the improved phasor ESC controller for the single variable case (with $\mathbf{z}=\begin{bmatrix}\beta_0 & \alpha_1 & \beta_1\end{bmatrix}^T=\begin{bmatrix}z_1 & z_2 & z_3\end{bmatrix}^T$). This yields

$$\frac{\mathrm{d}\mathbf{x}}{\mathrm{d}t}=\mathbf{f}\left(\mathbf{x},\gamma\left(\mathbf{x},\theta\left(t\right)+(a^2+a_0)\sin\left(\omega t\right)\right)\right) \tag{14a}$$

$$\frac{\mathrm{d}\mathbf{z}}{\mathrm{d}t}=\sqrt{\frac{q}{r}}L_g(\omega t)h\left(\mathbf{x}\right)-\sqrt{\frac{q}{r}}L_n(\omega t)C(\omega t)\mathbf{z} \tag{14b}$$

$$\frac{\mathrm{d}\theta}{\mathrm{d}t}=kz_2 \tag{14c}$$

$$\frac{\mathrm{d}a}{\mathrm{d}t}=-\lambda a+\lambda K_g\rho(z_2,z_3) \tag{14d}$$

where $C(\omega t)=\begin{bmatrix}1 & (a^2+a_0)\sin(\omega t) & (a^2+a_0)\cos(\omega t)\end{bmatrix}^T$ and $\rho(z_2,z_3)=\frac{2}{\pi}\tan^{-1}\left(\sqrt{z_2^2+z_3^2}\right)$.

The parameters of the controller will be selected as:

$$k=\omega K=\omega\delta K',\ \sqrt{\frac{q}{r}}=K_{q,r}=\omega\delta K'',\text{ and }\lambda=\omega\delta K_\lambda$$

where δ is a small positive number, and K', K'', as well as K_λ are $O(1)$ positive constants.

Introducing the time scale $\tau=\omega t$, results in

$$\omega\frac{\mathrm{d}\mathbf{x}}{\mathrm{d}\tau}=\mathbf{f}(\mathbf{x},\gamma(\mathbf{x},\theta+(a^2+a_0)\sin(\tau))) \tag{15a}$$

$$\frac{\mathrm{d}\mathbf{z}}{\mathrm{d}\tau} = \delta K'' \left(L_g(\tau)h(\mathbf{x}) - L_n(\tau)C(\tau)\mathbf{z}\right) \tag{15b}$$

$$\frac{\mathrm{d}\theta}{\mathrm{d}\tau} = \delta K' z_2 \tag{15c}$$

$$\frac{\mathrm{d}a}{\mathrm{d}\tau} = \delta\left(-K_\lambda a + K_\lambda K_g \rho(z_2, z_3)\right). \tag{15d}$$

Next, similar to the analysis of classic ESC [7], [16], we freeze $\mathbf{x}$ at its equilibrium value, that is, $\mathbf{x} = l(\theta_r + (a_r^2 + a_0)\sin(\tau))$ and $Q(\theta) = h(l(\theta))$. The reduced system can be seen as the fast dynamics and is then given by

$$\begin{aligned}\frac{\mathrm{d}\mathbf{z}_r}{\mathrm{d}\tau} =& \delta K'' \big(L_g(\tau)l(\theta_r + (a_r^2 + a_0)\sin(\tau)) \\ & - L_n(\tau)C(\tau)\mathbf{z}_r\big)\end{aligned} \tag{16a}$$

$$\frac{\mathrm{d}\theta_r}{\mathrm{d}\tau} = \delta K' z_{r2} \tag{16b}$$

$$\frac{\mathrm{d}a_r}{\mathrm{d}\tau} = \delta\left(-K_\lambda a + K_\lambda K_g \rho(z_{r2}, z_{r3})\right) \tag{16c}$$

where $\mathbf{z}_r = \begin{bmatrix} z_{r1} & z_{r2} & z_{r3}\end{bmatrix}^T$, θ_r, and a_r are the state variables of the reduced fast system. Now, (16) can be expanded and the averaged system can be calculated as [8]

$$\frac{\mathrm{d}z_{a1}}{\mathrm{d}\tau} = \delta K'' \left(\frac{1}{2\pi}\int_0^{2\pi} Q(\theta_a + (a_a^2 + a_0)\sin(\sigma))\mathrm{d}\sigma - z_{a1}\right) \tag{17a}$$

$$\begin{aligned}\frac{\mathrm{d}z_{a2}}{\mathrm{d}\tau} =& \delta K''\sqrt{2}\Bigg(\frac{\cos(\zeta)}{2\pi}\int_0^{2\pi} Q(\theta_a + (a_a^2 + a_0)\sin(\sigma))\bar{g}(\sigma)\mathrm{d}\sigma \\ & + \frac{\sin(\zeta)}{2\pi}\int_0^{2\pi} Q(\theta_a + (a_a^2 + a_0)\sin(\sigma))\bar{g}_c(\sigma)\mathrm{d}\sigma \\ & - (a_a^2 + a_0)\frac{\cos(\zeta)}{2} z_{a2} - (a_a^2 + a_0)\frac{\sin(\zeta)}{2} z_{a3}\Bigg)\end{aligned} \tag{17b}$$

$$\begin{aligned}\frac{\mathrm{d}z_{a3}}{\mathrm{d}\tau} =& \delta K''\sqrt{2}\Bigg(\frac{\cos(\zeta)}{2\pi}\int_0^{2\pi} Q(\theta_a + (a_a^2 + a_0)\sin(\sigma))\bar{g}_c(\sigma)\mathrm{d}\sigma \\ & - \frac{\sin(\zeta)}{2\pi}\int_0^{2\pi} Q(\theta_a + (a_a^2 + a_0)\sin(\sigma))\bar{g}(\sigma)\mathrm{d}\sigma \\ & + (a_a^2 + a_0)\frac{\sin(\zeta)}{2} z_{a2} - (a_a^2 + a_0)\frac{\cos(\zeta)}{2} z_{a3}\Bigg)\end{aligned} \tag{17c}$$

$$\frac{\mathrm{d}\theta_a}{\mathrm{d}\tau} = \delta K' z_{a2} \tag{17d}$$

$$\frac{\mathrm{d}a_a}{\mathrm{d}\tau} = \delta\left(-K_\lambda a_a + K_\lambda K_g \rho(z_{a2}, z_{a3})\right) \tag{17e}$$

where $\mathbf{z}_a = \begin{bmatrix} z_{a1} & z_{a2} & z_{a3}\end{bmatrix}^T$, θ_a, a_a are the state variables of the reduced and averaged fast system. Note that from [15] it is known that,

$$\int_0^{2\pi} Q(\theta_a + (a_a^2 + a_0)\sin(\sigma))\bar{g}_c(\sigma)\mathrm{d}\sigma = 0 \tag{18}$$

and hence, the corresponding terms in both (17b) and (17c) disappear. Next, let $\bar{\theta}_a = \theta_a - \theta^*$. Then, by using (13), the system (17) can be further rewritten as

$$\frac{\mathrm{d}z_{a1}}{\mathrm{d}\tau} = \delta K'' \left(\frac{1}{2\pi}\int_0^{2\pi} Q(\bar{\theta}_a + \theta^* + (a_a^2 + a_0)\sin(\sigma))\mathrm{d}\sigma - z_{a1}\right) \tag{19a}$$

$$\begin{aligned}\frac{\mathrm{d}z_{a2}}{\mathrm{d}\tau} =& \delta K''\sqrt{2}(a_a^2 + a_0)\Bigg(\frac{\cos(\zeta)}{2}Q'(\bar{\theta}_a + \theta^*) \\ & - \frac{\cos(\zeta)}{2} z_{a2} - \frac{\sin(\zeta)}{2} z_{a3}\Bigg)\end{aligned} \tag{19b}$$

$$\begin{aligned}\frac{\mathrm{d}z_{a3}}{\mathrm{d}\tau} =& \delta K''\sqrt{2}(a_a^2 + a_0)\Bigg(-\frac{\sin(\zeta)}{2}Q'(\bar{\theta}_a + \theta^*) \\ & + \frac{\sin(\zeta)}{2} z_{a2} - \frac{\cos(\zeta)}{2} z_{a3}\Bigg)\end{aligned} \tag{19c}$$

$$\frac{\mathrm{d}\bar{\theta}_a}{\mathrm{d}\tau} = \delta K' z_{a2} \tag{19d}$$

$$\frac{\mathrm{d}a_a}{\mathrm{d}\tau} = \delta\left(-K_\lambda a_a + K_\lambda K_g \rho(z_{a2}, z_{a3})\right) \tag{19e}$$

Remark 4: The system in (19) provides insight about the effect of increasing the amplitude: It can be seen that the right hand sides of (19b) and (19c) scale with factor $a_a^2 + a_0$. This implies that the larger $a_a^2 + a_0$, the faster α_1 and β_1 are estimated.

The averaged system (19) is a cascaded system: The combined system (19b)-(19e) can be seen as an input to the input-to-state stable system (19a). Thus, let us define the following Lyapunov function candidate with $\chi = \begin{bmatrix} z_{a2} & z_{a3} & \bar{\theta}_a & a_a\end{bmatrix}^T$:

$$\begin{aligned}V(\chi) =& 0.5\chi^T P(\zeta, \mu, a_a)\chi \\ & - \frac{K''\cos(2\zeta)(a_a^2 + a_0)\left(Q(\bar{\theta}_a + \theta^*) - Q(\theta^*)\right)}{\sqrt{2}K'}\end{aligned} \tag{20}$$

and note that $Q(\bar{\theta}_a + \theta^*) < Q(\theta^*)\ \forall\ \bar{\theta}_a \neq \theta^*$ and that $\cos(2\zeta) > 0$ if $0 \leq \zeta < \frac{\pi}{4}$. $P(\zeta, \mu, a)$ is given by

$$P(\zeta,\mu,a) = \begin{bmatrix} \cos(\zeta) & \sin(\zeta) & \frac{\sqrt{2}\mu K''}{K'} & 0 \\ \sin(\zeta) & \cos(\zeta) & -\frac{\sqrt{2}\mu K''\sin(\zeta)}{K'\cos(\zeta)} & 0 \\ \frac{\sqrt{2}\mu K''}{K'} & -\frac{\sqrt{2}\mu K''\sin(\zeta)}{K'\cos(\zeta)} & \frac{\mu K''^2(a_a^2 + a_0)}{K'^2\cos(\zeta)} & 0 \\ 0 & 0 & 0 & \frac{1}{K_\lambda}\end{bmatrix}.$$

Let

$$M_1(\zeta,\mu) = \begin{bmatrix} a_0\cos(2\zeta) - 2\mu & \frac{\mu\sin(\zeta)}{\cos(\zeta)} + \frac{a_0\sin(\zeta)}{2} \\ \frac{\mu\sin(\zeta)}{\cos(\zeta)} + \frac{a_0\sin(\zeta)}{2} & a_0\end{bmatrix},$$

$$M_2(\zeta) = \begin{bmatrix} \cos(2\zeta) & \frac{\sin(2\zeta)}{2} \\ \frac{\sin(2\zeta)}{2} & 1\end{bmatrix},$$

and

$$\begin{aligned}M_3(\zeta,\mu) =& \frac{\sqrt{2}\mu K'' K_\lambda}{K'^2\cos(\zeta)}\theta^2 + \frac{2}{\sqrt{2}K''} \\ & - \frac{4\cos(2\zeta)K_\lambda\left(Q(\bar{\theta}_a + \theta^*) - Q(\theta^*)\right)}{K'}\end{aligned}$$

and note that $M_3(\zeta,\mu)$ is positive since $Q(\bar{\theta}+\theta^*) - Q(\theta^*) < 0 \ \forall \ \theta \neq \theta^*$. Then, it can be shown that

$$
\begin{aligned}
\frac{2}{\sqrt{2}K''\delta}\frac{\partial V(\chi)}{\partial \chi} f(\chi) \\
&= -\begin{bmatrix} z_{a2} & z_{a3} \end{bmatrix}\left(M_1(\zeta,\mu) + a_a^2 M_2(\zeta)\right)\begin{bmatrix} z_{a2} \\ z_{a3} \end{bmatrix} \\
&\quad + \frac{\mu K''(a_a^2 + a_0)}{K'\cos(\zeta)}\bar{\theta}_a Q'(\bar{\theta}_a + \theta^*) \\
&\quad - \left(a_a^2 - a_a K_g \rho(z_{a2}, z_{a3})\right) M_3(\zeta,\mu).
\end{aligned}
$$

The eigenvalues of $M_1(\zeta,\mu)$ for $\mu \to 0$ are $a_0 e_{min}$ and $a_0 e_{max}$ where

$$
e_{min} = \cos(\zeta)^2 - \sin(\zeta)\frac{\sqrt{4\sin(\zeta)^2 + 1}}{2}
$$

and

$$
e_{max} = \cos(\zeta)^2 + \sin(\zeta)\frac{\sqrt{4\sin(\zeta)^2 + 1}}{2},
$$

while the eigenvalues of $M_2(\zeta)$ are e_{min} and e_{max}. Moreover, similar as in [16], it can be shown that for sufficiently small μ, any $\zeta < \zeta_0 = 0.5\cos^{-1}\left(\sqrt{5}-2\right) \approx 38.17°$ will make $P(\zeta,\mu,a)$, and consequently also $M_1(\zeta,\mu)$ and $M_2(\zeta)$ positive definite. Hence, we have that

$$
\begin{aligned}
\frac{2}{\sqrt{2}K''\delta}\frac{\partial V(\chi)}{\partial \chi} f(\chi) \leq &-\left(a_0 + a_a^2\right) e_{min} \|[z_{a2}, z_{a3}]\|^2 \\
&+ \frac{\mu K''(a_a^2 + a_0)}{K'\cos(\zeta)}\bar{\theta}_a Q'(\bar{\theta}_a + \theta^*) \\
&- \left(a_a^2 - a_a K_g \rho(z_{a2}, z_{a3})\right) M_3(\zeta,\mu).
\end{aligned} \tag{21}
$$

Since $\rho(z_2,z_3) = \frac{2}{\pi}\tan^{-1}\left(\sqrt{z_2^2 + z_3^2}\right) \leq \frac{2}{\pi}\| \begin{bmatrix} z_2 & z_3 \end{bmatrix} \|$ we can, based on the inequality $x^2 + y^2 \geq xy$, guarantee that $a_a^2 - a_a K_g \rho(z_{a2}, z_{a3})$ is positive definite. Thus, by choosing $K_g \frac{2}{\pi} \leq \sqrt{a_0 \, e_{min}}$, we can make sure that that the entire right hand side of the Lyapunov equation will be positive definite. Finally, the system (19b)-(19e)) is globally asymptotically stable (GAS) and, in combination with the fact that (19a) is input-to-state stable, the averaged system (19) is GAS also.

In conjunction with [16, Lemma 1], (16) is thus SPA stable in $\begin{bmatrix} \bar{a} & \zeta & \delta & K_\lambda & K_g \end{bmatrix}^T$ uniformly in $\begin{bmatrix} \bar{a} & \zeta \end{bmatrix}^T$. Hence, we can postulate the following theorem based on [7, Lemma 1].

Theorem 1: Suppose that Assumptions 1, 2, and 3 hold. Then, the closed-loop system (15) with parameters $\begin{bmatrix} a & \zeta & \delta & K_\lambda & K_g & \omega \end{bmatrix}^T$ is SPA stable, uniformly in $\begin{bmatrix} a & \zeta \end{bmatrix}^T$ with the time scale t.

Remark 5: If the standard phasor ESC will be used (that is, $\bar{m} = 0$), a similar result can be obtained by approximating the integration of (13) to yield the same right hand side by using the approximation presented in [7, Eq. (44)]. Thus, the approximated averaged system will be GAS, and the non-approximated averaged system will be SPA, and using [17, Lemma 1] can be used to prove that the reduced system is SPA too.

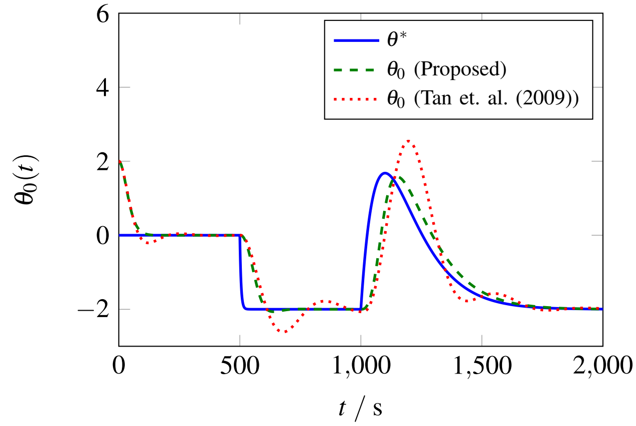

Fig. 2. Illustration of the perturbation-free control signal $\theta_0(t)$: The true optimal signal θ^* (blue, solid) together with the signal of the proposed approach (green, dashed), and the approach by [6] (red, dotted).

VI. Simulation

In this section, we provide a numerical illustration of the proposed method where we compare the proposed adaptive phasor ESC to classic ESC with a constant decay rate of the perturbation amplitude as proposed by [6].

A. Simulation Model

The system under consideration is given by the non-linear, time-varying state-space model

$$
\dot{x} = -10x + \theta - \theta^*(t) \tag{22a}
$$

$$
y = -x^2 \tag{22b}
$$

where

$$
\theta^*(t) = \begin{cases} 0 & 0 \leq t < 500 \\ -2\left(1 - \mathrm{e}^{-5(t-500)}\right) & 500 \leq t < 1000 \\ -2 + 0.1\left(t - 10^3\right)\mathrm{e}^{-0.01\left(t-10^3\right)} & 1000 \leq t \end{cases}.
$$

It follows that the steady-state map of this system is $Q(\theta) = -(\theta - \theta^*(t))^2$ which has a maximum $y^* = 0$ at $\theta^*(t)$.

The parameters used in the simulations are $\omega = 2\,\mathrm{rad/s}$ for the perturbation signal frequency, $\frac{q}{r} = 1$, $\zeta = \frac{\pi}{8}$, $a_0 = 0.025$, $a(0) = 0.25$, $\theta_0(0) = 2$, $k = 0.025$, and $\lambda = 0.0025$ for both approaches. For the proposed approach, $K_g = 1.5$ was chosen, while for the comparison, $K_g = 0$ (as per definition).

B. Results and Discussion

The results are shown in Fig. 2-Fig. 4. From Fig. 2, it can be seen that the proposed approach (green, dashed line) is able to track the optimum θ^* accurately (blue, solid). Comparing it to the method with exponentially decaying amplitude [6] (red, dotted), we see that the two methods perform similarly in the beginning during the start-up phase. However, once the amplitude of the latter approach has decayed to a minimum, it is not able to track changes in the optimal point as quickly as the proposed method (see the changes at $t = 500\,\mathrm{s}$ and $t = 1000\,\mathrm{s}$.)

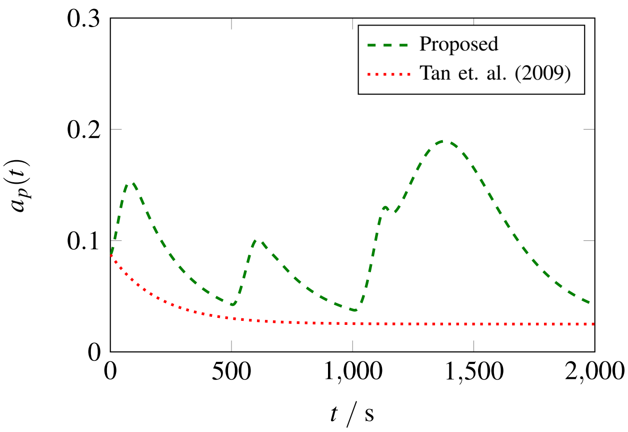

Fig. 3. Illustration of the perturbation amplitude $a_p(t)$: The proposed approach (green, dashed) and the approach by Tan et. al. [6] (red, dotted).

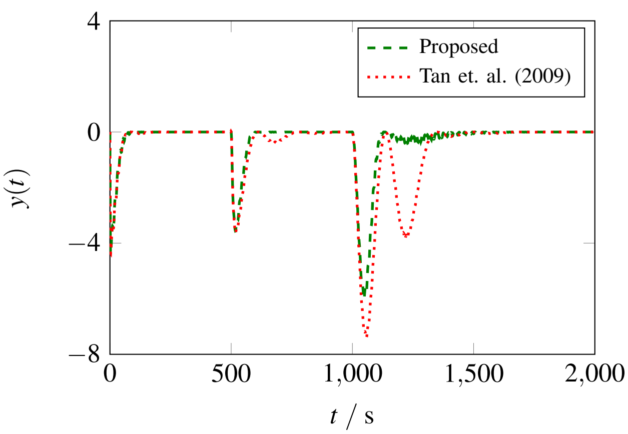

Fig. 4. Illustration of the plant output $y(t)$: The proposed approach (green, dashed), as well as the approach with exponential decay [6] (red, dotted).

The adaption of the perturbation amplitude is illustrated in Fig. 3. As can be seen, the proposed method adapts the perturbation amplitude as desired. If there is no change in the optimum point, the amplitude decays in order to minimize the unnecessary oscillations around the working point. However, once the optimum point changes, the amplitude is increased quickly in order to track the change (green, dashed). In contrast, with the exponential decay approach (red, dotted) the amplitude decays to its minimum value with time and remains there, which makes it respond more slowly to changes.

Finally, the behavior of the plant output $y(t)$ is depicted in Fig. 4. As can be seen from the figure, the proposed approach is able to drive the plant to optimality quickly and without much overshoot (green, dashed). The negative overshoot in the approach by Tan et. al. [6] can be explained by comparing the output to the control signal shown in Fig. 2: The negative dip in the output is caused by the lagging control signal $\theta(t)$ which has a peak when the optimal control signal θ^* is decaying (around $t = 1250\,\mathrm{s}$).

VII. Conclusion and Future Work

In this work, an adaptive perturbation amplitude phasor extremum seeking control strategy was suggested. It was proven that the method is semi-globally, practically asymptotically stable. Furthermore, simulations illustrated that it is able to track changes in the optimal point quickly while reducing the perturbation amplitude to a minimum when in steady-state.

Future development of this work will include an analysis of the connection between adaptive amplitude (both classical and phasor) ESC and disturbance rejection. In particular, it is of interest to analyze how robust the proposed methods are toward both vanishing and non-vanishing disturbances as well as measurement noise which is always present in real world applications. Furthermore, a natural extension of the proposed method will be vanishing perturbation ESC, that is, it will be investigated whether we can develop robust ESC with a vanishing dither signal. We are also planning to evaluate the practical applicability of the proposed method by applying it to a district heating and cooling system.

References

[1] Y. Tan, W. Moase, C. Manzie, D. Nesic, and I. Mareels, "Extremum seeking from 1922 to 2010," in *Control Conference (CCC), 2010 29th Chinese*, 2010, pp. 14–26.

[2] M. Krstić and H. Wang, "Stability of extremum seeking feedback for general nonlinear dynamic systems," *Automatica*, vol. 36, no. 4, pp. 595–601, 2000.

[3] W. Moase, C. Manzie, and M. Brear, "Newton-like extremum-seeking for the control of thermoacoustic instability," *Automatic Control, IEEE Transactions on*, vol. 55, no. 9, pp. 2094–2105, 2010.

[4] K. T. Atta, A. Johansson, and T. Gustafsson, "Extremum seeking control based on phasor estimation," *Systems & Control Letters*, vol. 85, pp. 37–45, 2015.

[5] K. T. Atta, A. Johansson, M. J. Cervantes, and T. Gustafsson, "Phasor extremum seeking and its application in kaplan turbine control," in *Control Applications (CCA), 2014 IEEE Conference on*. IEEE, 2014, pp. 298–303.

[6] Y. Tan, D. Nešić, I. M. Mareels, and A. Astolfi, "On global extremum seeking in the presence of local extrema," *Automatica*, vol. 45, no. 1, pp. 245–251, 2009.

[7] Y. Tan, D. Nešić, and I. Mareels, "On non-local stability properties of extremum seeking control," *Automatica*, vol. 42, no. 6, pp. 889–903, 2006.

[8] H. K. Khalil, *Nonlinear systems*. Prentice Hall, 2002, vol. 3.

[9] M. Chioua, B. Srinivasan, M. Guay, and M. Perrier, "Dependence of the error in the optimal solution of perturbation-based extremum seeking methods on the excitation frequency," *The Canadian Journal of Chemical Engineering*, vol. 85, no. 4, pp. 447–453, 2007.

[10] A. Gelb, *Applied optimal estimation*. MIT Press, 1974.

[11] A. C. Harvey, *Forecasting, structural time series models and the Kalman filter*. Cambridge University Press, 1990.

[12] A. A. Girgis, W. B. Chang, and E. B. Makram, "A digital recursive measurement scheme for online tracking of power system harmonics," *Power Delivery, IEEE Transactions on*, vol. 6, no. 3, pp. 1153–1160, 1991.

[13] G. E. Box, G. M. Jenkins, and G. Reinsel, *Time Series Analysis, Forecast and Contral*. Prentice Hall, 1994.

[14] K. T. Atta, A. Johansson, and T. Gustafsson, "Control oriented modeling of flow and size distribution in cone crushers," *Minerals Engineering*, vol. 56, pp. 81–90, 2014.

[15] ——, "Accuracy improvement of extremum seeking control," *IEEE Transactions on Automatic Control*, 2016, accepted for publication.

[16] ——, "On the stability analysis of phasor and classic extremum seeking control," *Systems & Control Letters*, vol. 91, pp. 55–62, 2016.

[17] Y. Tan, D. Nešić, and I. Mareels, "On non-local stability properties of extremum seeking control," in *Proceedings of the 16th IFAC World Congress, 2005*, 2005, pp. 746–746.